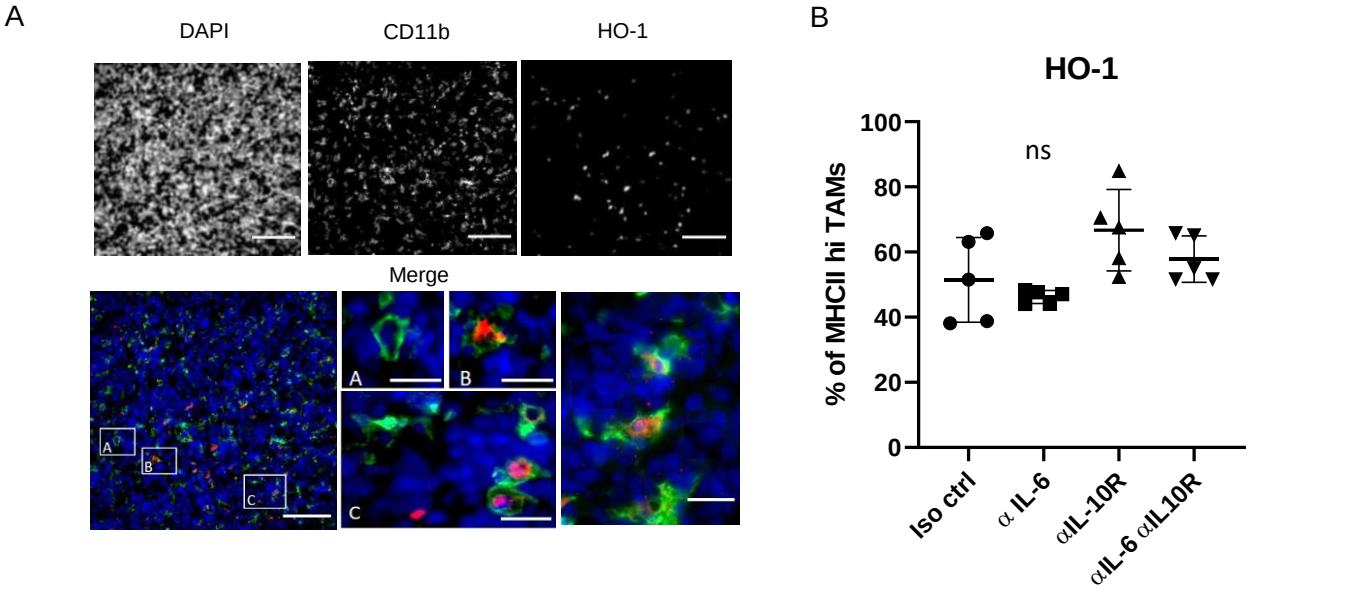

Supplemental Figure 1. HO-1 expression by TAMs. A) HO-1 staining (in red) combined with DAPI co-staining showing nuclei (in blue) are visualized in tumor slices by immunofluorescence in CD11b^{+} myeloid cells (in green) in an EG7-OVA tumor 21 days after tumor inoculation in a wild type mouse. Scale bar = 5 µm. B) HO-1 expression measured by flow cytometry among CD11b^{hi}Ly6G^{-}Ly6C^{lo}CD64^{+}MHCII^{+} TAMs from EG7-OVA tumor 16 days after inoculation in wild type mice, after in vivo neutralization of IL-6, IL-10, or both (n=5). *P<0,05; **P<0,01; ***P<0,001; ****P<0,0001, ns: not significant. .Kruskall-Wallis and Dunn's multiple comparisons test.

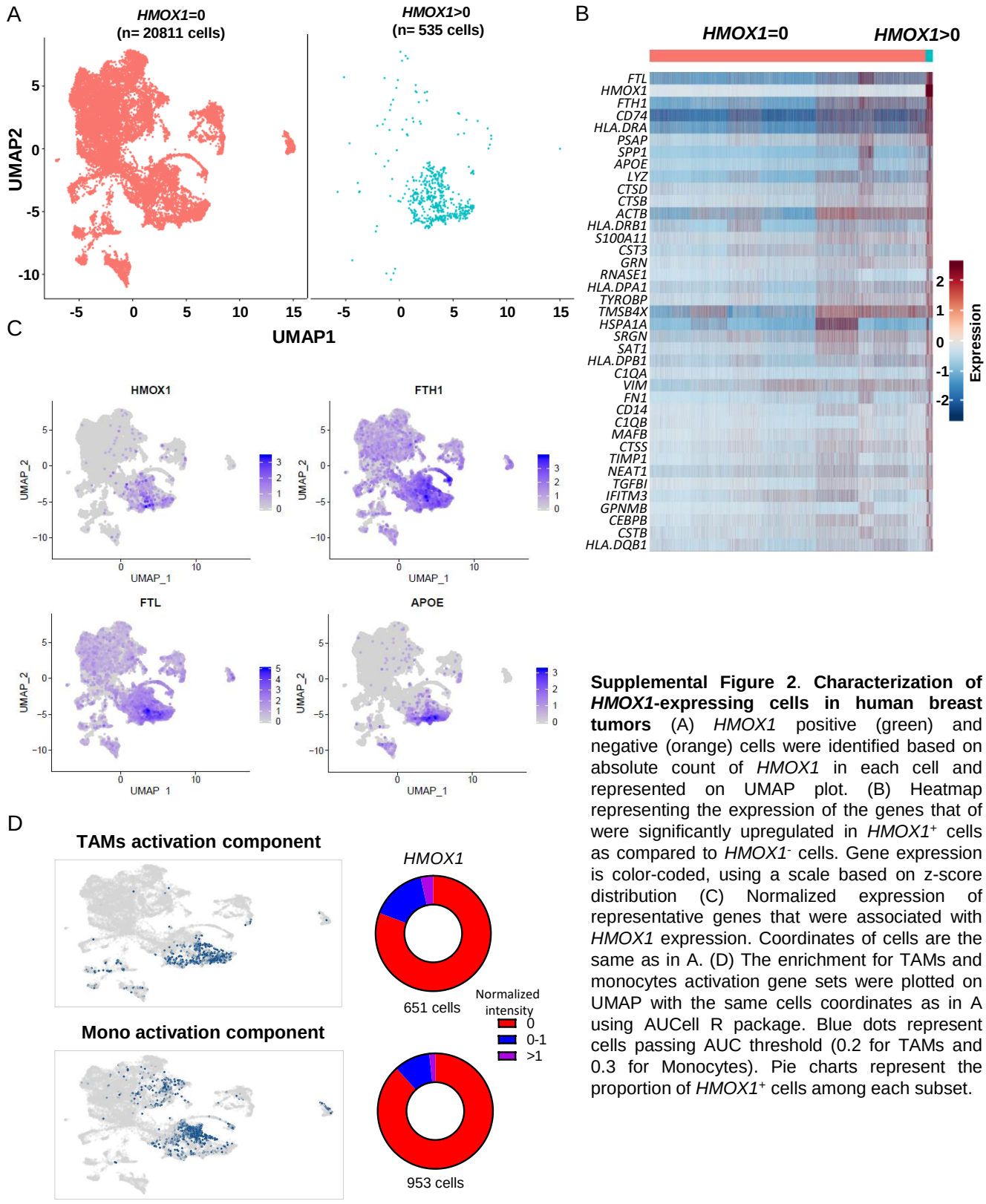

Supplemental Figure 2. Characterization of *HMOX1*-expressing cells in human breast tumors (A) *HMOX1* positive (green) and negative (orange) cells were identified based on absolute count of *HMOX1* in each cell and represented on UMAP plot. (B) Heatmap representing the expression of the genes that of were significantly upregulated in *HMOX1*$^{+}$ cells as compared to *HMOX1*$^{-}$ cells. Gene expression is color-coded, using a scale based on z-score distribution (C) Normalized expression of representative genes that were associated with *HMOX1* expression. Coordinates of cells are the same as in A. (D) The enrichment for TAMs and monocytes activation gene sets were plotted on UMAP with the same cells coordinates as in A using AUCell R package. Blue dots represent cells passing AUC threshold (0.2 for TAMs and 0.3 for Monocytes). Pie charts represent the proportion of *HMOX1*$^{+}$ cells among each subset.

Figure S3

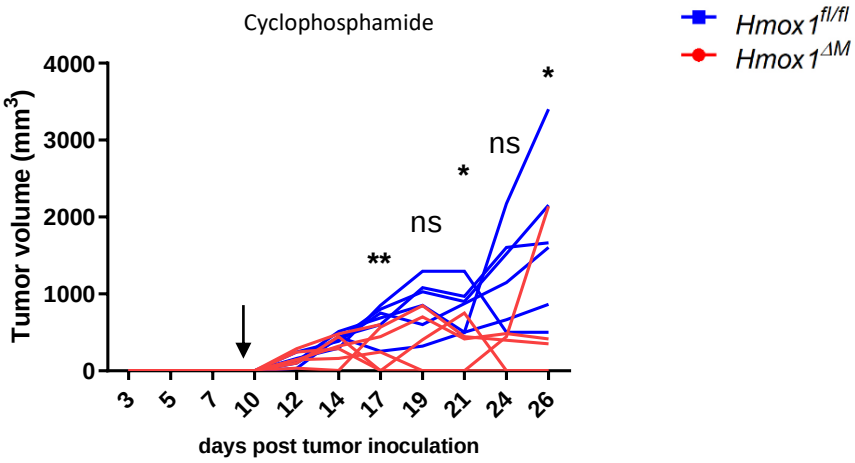

Supplemental Figure 3. Myeloid HO-1 inhibition improves the antitumor effect of cyclophosphamide treatment. EG7-OVA tumor cells were inoculated intradermally at day 0 on the right flank of *Hmox1$^{\Delta M}$ mice* (n = 6). All mice were injected with cyclophosphamide (i.p.) at day 10 post tumor inoculation. Their tumor volumes were compared to *Hmox1$^{fl/fl}$* littermates (n = 6) at regular intervals following implantation. Statistical analysis was performed with Mann-Whitney U test. *P<0,05; **P<0,01; ***P<0,001; ****P<0,0001.

Figure S4

A

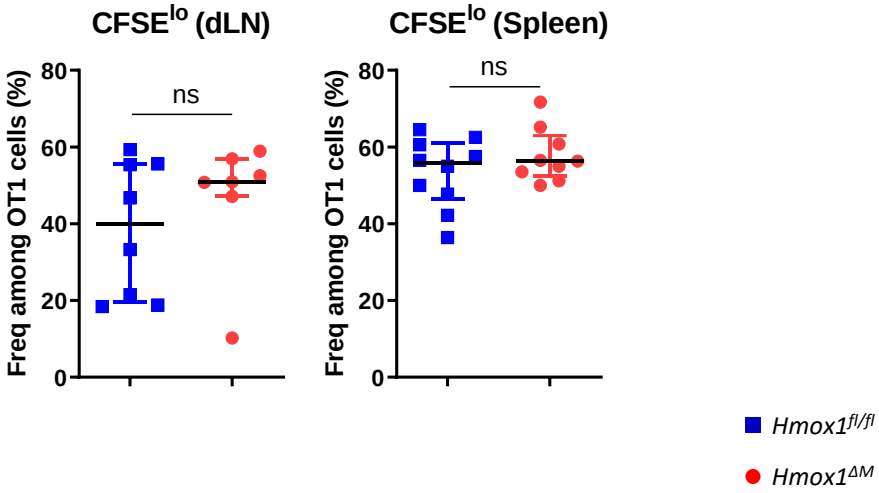

B

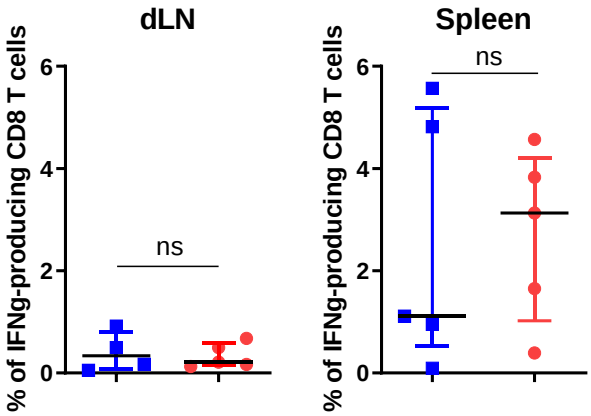

Supplemental Figure 4. Myeloid HO-1 inhibition has no impact on T-cell priming in the secondary lymphoid organs. Intravenous adoptive transfer of CFSE labelled OT-1 cells ($2x10^6$ cells/mouse) was performed 10 days after tumor inoculation. This was followed by an immunization with subcutaneous injection of ovalbumin protein (50 µg/mouse) and poly(I:C) (50 µg/mouse) one hour later on the right flank of the animals. Two days later, EG7-OVA tumors were enzymatically and mechanistically digested and analyzed by flow cytometry. A) Tumor-infiltrating OT-1 cell proliferation assessed by CFSE dilution in the axillary and inguinal draining lymph nodes on the right flank and the spleen of *Hmox1*$^{\Delta M}$ mice and *Hmox1*$^{fl/fl}$ littermates mice. dLN: n=8 (littermates) or n=7 (*Hmox1*$^{\Delta M}$ *mice)*. Spleen: n=10 (littermates) or n=9 (*Hmox1*$^{\Delta M}$ *mice)*. B) Production of IFNɤ was assessed by ex vivo stimulation overnight with OVA SIINFEKL peptide (and brefeldin A added 2 hours later). dLN: n=4 (littermates) or n=5 (*Hmox1*$^{\Delta M}$ *mice)*. Spleen: n=5 (littermates) or n=5 (*Hmox1*$^{\Delta M}$ *mice)*. Horizontal bars indicate median ± interquartile. Statistical analysis was performed with Mann-Whitney U test. *P<0,05; **P<0,01; ***P<0,001; ****P<0,0001.